

The role of compressional Pc5 pulsations in modulating precipitation of energetic electrons

T. Motoba,¹ K. Takahashi,¹ J. Gjerloev,^{1,2} S. Ohtani,¹ and D. K. Milling³

Received 1 April 2013; revised 4 November 2013; accepted 29 November 2013; published 26 December 2013.

[1] Pc5 (1.67–6.67 mHz) magnetic pulsations and the modulation of energetic electron precipitation are often observed simultaneously in the morning auroral-latitude data. Here we have investigated a conjunction event of Cluster spacecraft and Canadian auroral-latitude ground stations to identify the role of compressional Pc5 pulsations in modulating precipitation of energetic electrons observed by ground-based riometers. On 7 December 2002 as the spacecraft moved between $L = 4.0$ and 6.5 in the dawn sector (0600–0700 magnetic local time (MLT)), we found a monochromatic Pc5 magnetic pulsation at ~ 4.0 mHz simultaneously in space and on the ground. Both Cluster and ground magnetometer data confirmed that the resonant oscillation at 4.0 mHz occurred around $L = \sim 6.0$. Simultaneously, the four Cluster spacecraft identified the compressional Pc5, which was accompanied by similar temporal variations of the fluxes of medium energy (tens to hundreds of keV) electrons and of the intensity of whistler mode chorus waves. While the compressional Pc5 was present in the magnetosphere, the riometers near the spacecraft footprint observed the coincident modulation of electron precipitation at ~ 4.0 mHz. Our coordinated observations indicate a convincing relationship between compressional Pc5 magnetic pulsations in the magnetosphere and the modulation of electron precipitation in the ionosphere, mediated by chorus waves modulated in the magnetosphere, as predicted by the theory of *Coroniti and Kennell* [1970]. Around the resonant shell, however, some additional contributions to the modulation of electron precipitation might also come from the effects of the resonant Pc5 oscillation.

Citation: Motoba, T., K. Takahashi, J. Gjerloev, S. Ohtani, and D. K. Milling (2013), The role of compressional Pc5 pulsations in modulating precipitation of energetic electrons, *J. Geophys. Res. Space Physics*, 118, 7728–7739, doi:10.1002/2013JA018912.

1. Introduction

[2] Whistler mode chorus waves, in the frequency range from a few hundreds of Hz to several kHz, cause pitch angle scattering of energetic electrons into the loss cone leading to precipitation losses into the ionosphere/atmosphere [*Kennel and Petschek*, 1966]. Chorus waves typically occur in two distinct frequency bands, a lower band with frequencies of $0.1\text{--}0.5 f_{ce}$ and an upper band with frequencies of $0.5\text{--}1.0 f_{ce}$, where f_{ce} is the electron cyclotron frequency. The lower band chorus tends to provide more effective scattering electrons with higher energies more than several tens of keV, whereas the upper band chorus contributes to the scattering loss of electrons below 5 keV [*Ni et al.*, 2008].

[3] When the amplitude of chorus waves changes periodically, the precipitation of energetic electrons will also change

on the same timescale. Indeed, a periodic nature of electron precipitation can be observed by a ground-based riometer, recording cosmic noise absorption (CNA) that is an indicator of precipitation of energetic electrons into the lower ionosphere. Typical periods of the CNA pulsations range from a few seconds to several minutes associated with ultralow frequency (ULF, frequency range from 1 mHz to 1 Hz) magnetic pulsations [e.g., *Barcus and Rosengerg*, 1965; *Reid*, 1976; *Rosenberg et al.*, 1979]. *Coroniti and Kennell* [1970] proposed a possible mechanism for how magnetospheric ULF magnetic pulsations modulate the precipitation of electrons. The hypothesis suggests that periodic change in the local magnetic field strength due to the ULF pulsations modulates the growth rate of whistler mode chorus waves and the associated rate of electron pitch angle scatter. Consequently, the electrons undergo a variation in the strength of pitch angle diffusion from a background state at the same frequency as the ULF pulsations, which in turn will lead to periodic changes in precipitation as the amount of loss cone filling is modulated.

[4] Pc5 range (1.67–6.67 mHz, 150–600 s) ULF pulsations, which are the focus of the present study, are well known to preferentially occur in the morning (0600–1200 MLT) auroral zone [e.g., *Baker et al.*, 2003]. The spatial distribution partially overlaps with that of the precipitating energetic electrons and chorus waves primarily seen in $L = 4\text{--}7$ outside of the

¹Johns Hopkins University Applied Physics Laboratory, Laurel, Maryland, USA.

²Birkeland Centre, University of Bergen, Bergen, Bergen, Norway.

³Department of Physics, University of Alberta, Edmonton, Alberta, Canada.

Corresponding author: T. Motoba, Johns Hopkins University Applied Physics Laboratory, 11100 Johns Hopkins Rd., 200-E274, Laurel, MD 20723–6099, USA. (tetsuo.motoba@gmail.com)

Table 1. Location of the CANOPUS Magnetometers and NORSTAR Riometers^a

Station	Geographic Latitude	Longitude	AACGM Latitude	Longitude	L Value	MLT
Taloyoak (TAL)	69.54°	266.45°	78.59°	330.10°	N/A	UT – 06:57
Rankin Inlet (RAN)	62.82°	267.89°	72.57°	335.37°	11.1	UT – 06:36
Eskimo Point (ESK)	61.11°	265.95°	70.85°	332.54°	9.3	UT – 06:47
Fort Churchill (CHU)	58.76°	265.92°	68.64°	332.97°	7.5	UT – 06:45
Gillam (GIL)	56.38°	265.36°	66.34°	332.51°	6.2	UT – 06:46
Island Lake (ISL)	53.86°	265.34°	63.91°	332.84°	5.2	UT – 06:52
Pinawa (PIN)	50.20°	263.96°	60.22°	331.23°	4.1	UT – 06:43
Rabbit Lake (RAB)	58.22°	256.32°	67.07°	318.42°	6.6	UT – 07:23
Fort McMurray (MCM)	56.66°	248.79°	64.30°	308.51°	5.3	UT – 08:23
Fort Smith (FSM)	60.02°	248.05°	67.46°	306.17°	6.8	UT – 08:32
Fort Simpson (FSI)	61.76°	238.77°	67.35°	293.51°	6.7	UT – 09:23
Dawson City (DAW)	64.05°	220.89°	65.95°	273.16°	6.0	UT – 10:45

^aThe geomagnetic latitude and longitude and magnetic local time (MLT) are represented in the Altitude Adjusted Corrected GeoMagnetic (AACGM) coordinates.

plasmopause on the dawnside [e.g., *Lam et al.*, 2010]. The ground Pc5 magnetic pulsations are sometimes accompanied by the CNA pulsations [e.g., *Olson et al.*, 1980; *Poulter and Nielsen*, 1982], VLF emissions (called “QP emissions”) [e.g., *Kimura*, 1974], or both [e.g., *Sato et al.*, 1985; *Paquette et al.*, 1994; *Manninen et al.*, 2010] with a high degree of correlation. Such an interrelationship between Pc5 magnetic pulsations and CNA pulsations and/or QP emissions provided further supporting evidence for the *Coroniti and Kennell* [1970] theory.

[5] Recently, *Spanswick et al.* [2005] investigated in details the morphology of auroral-latitude Pc5 CNA pulsations and their relationship to Pc5 magnetic pulsations, based on a detailed statistical survey of long-term data sets from the CANOPUS magnetometer and NORSTAR riometer arrays covering a time span of about 10 years. They found that both Pc5 magnetic and CNA pulsations occur preferentially on the dawnside (specifically, ~95% of their CNA pulsations occurred between 6 and 12 MLT); almost all CNA pulsations have a corresponding magnetic pulsation, and Pc5 magnetic pulsations with field line resonance (FLR) [*Southwood*, 1974; *Chen and Hasegawa*, 1974] signatures are more effective in modulating energetic electron precipitation than Pc5 magnetic pulsations without FLR signatures. In addition, they noted that the reverse is not true: Not all Pc5 geomagnetic pulsations are accompanied by a CNA pulsation. This meant that the presence of Pc5 magnetic pulsations on the ground is a necessary but not sufficient condition for CNA pulsations.

[6] Despite a large number of simultaneous observations using ground-based instruments, there have been few spacecraft observations unambiguously demonstrating the role of magnetospheric Pc5 pulsations in modulating the electron precipitation. Especially, using ground-based magnetometer data only, it is impossible to explicitly distinguish which modes of Pc5 magnetic pulsations in the magnetosphere govern the modulation of electron precipitation measured by riometers.

[7] In this paper, we present the first comprehensive study of the relationships among magnetospheric Pc5, whistler mode chorus waves, and electron precipitation, by combining simultaneous observations made in space and on the ground. We focus here on the interaction of Pc5 with energetic electrons observed at 1245–1315 UT on 7 December 2002, observed by the Cluster spacecraft. The spacecraft observed the Pc5 geomagnetic pulsations during a perigee

pass at $L \sim 4.0$ – 6.5 just outside the plasmopause. The ground-based magnetometers and riometers, located near the magnetic footprints of spacecraft, provided vital measurements of Pc5 magnetic and CNA pulsations associated with the modulation of the energetic electron flux and chorus wave intensity by magnetospheric Pc5 pulsations observed at the spacecraft. The remainder of the paper is organized as follows: in section 2 we describe the data set of space- and ground-based instruments used in this study, in section 3 we present the results of the data analysis, in section 4 we present the discussion, and finally, we provide the summary in section 5.

2. Data Set

[8] We use data from five instruments onboard Cluster (“CL” for short). These are the FluxGate Magnetometer (FGM) [*Balogh et al.*, 2001], Electric Field Wave (EFW) experiment [*Gustafsson et al.*, 2001], the Cluster Ion Spectrometry-Hot Ion Analyzer/Composition and Distribution Function Analyzer (CIS-HIA/CODIF) [*Rème et al.*, 2001], the Research with Adaptive Particle Imaging Detectors (RAPID) [*Wilken et al.*, 2001], and the Spatio Temporal Analysis of Field Fluctuations-Spectrum Analyzer (STAFF-SA) [*Cornilleau-Wehrin et al.*, 2003]. The RAPID is capable of detecting electrons in the energy range of 40–400 keV. The STAFF-SA provides five components of the electromagnetic field in the frequency range from 8 Hz to 4 kHz, three components of the magnetic field obtained from the magnetic search coils, and two components of the electric field from the sensors of the EFW experiment. The time resolution of each instrument is ~4 s, except the STAFF instrument with temporal resolution of 1 s. Note that the CIS instrument was not operational on CL2, and the CIS-HIA was switched off on CL4. In order to obtain the electric field vector (\mathbf{E}), we calculated the unmeasured third component (i.e., the z component) from the EFW instrument data through the assumption of $\mathbf{E} \cdot \mathbf{B} = 0$. At CL3 and CL4, however, there existed some data gaps, corresponding to the region where the assumption was not justified since the angle between the spin plane and magnetic field direction is $< 15^\circ$. For filling such data gaps at CL3 and CL4, we also used the components calculated from the cross product (i.e., $\mathbf{E} = -(\mathbf{V} \times \mathbf{B})$) of the magnetic field vector (\mathbf{B}) and ion (H^+ from CIS-CODIF for CL4) velocity vector (\mathbf{V}).

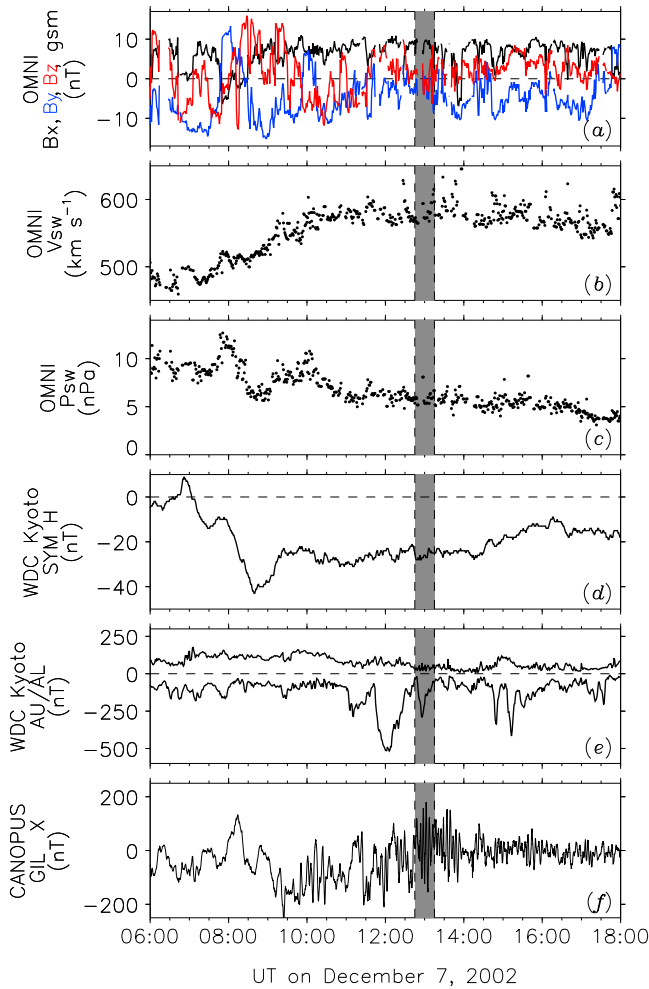


Figure 1. An overview of the solar wind condition, geomagnetic activity, and geomagnetic pulsations for 0600–1800 UT on 7 December 2002 covering the selected Pc5 event. (a–c) Three components of IMF (B_x : black, B_y : blue, B_z : red), solar wind speed (V_{sw}), and solar wind dynamic pressure (P_{sw}) from the high-resolution OMNI data (shifted to the bow shock nose). (d and e) $SYM-H$ index and provisional AU/AL indices from the World Data Center for Geomagnetism, Kyoto. (f) The X component of the ground-based magnetometer data from the Gillam (GIL, $L=6.2$) station of CANOPUS. The time interval of our interest is shaded by dark grey.

[9] For our analysis, the electric and magnetic field vectors are projected to the local mean field-aligned (FA) coordinate system [e.g., Takahashi *et al.*, 1990], to separate the Pc5 fluctuations into the compressional, toroidal, and poloidal modes. This coordinate system has the radial, azimuthal, and parallel components (e_r, e_ϕ, e_μ): the parallel unit vector e_μ is along the 15 min running average magnetic field vector, the azimuthal unit vector e_ϕ (positive is eastward) is in the direction of $e_\mu \times r$ (where r is the position vector of the satellite from the Earth’s center), and then the radial unit vector e_r completes the right-hand orthogonal set (radially outward at the magnetic equator). In the transformation into this coordinate system, the 15 min running average behaves as a high-pass filter removing frequencies below 1.1 mHz.

[10] The ground-based magnetometer and riometer data (temporal resolution of 5 s) used in this study are from the Canadian Auroral Network for the OPEN Program Unified Study (CANOPUS) array [Rostoker *et al.*, 1995] and the Northern Solar Terrestrial ARray (NORSTAR: formerly operated under the CANOPUS program), respectively. The CANOPUS magnetometer array is currently operated as the Canadian Array for Realtime InvestigationS of Magnetic Activity [Mann *et al.*, 2008]. Table 1 gives the station locations. The CANOPUS magnetometer data record the magnetic field in the geographic coordinate system, defined by the X (north–south), Y (east–west), and Z (vertical) components. Each NORSTAR riometer consists of a 30 MHz zenith-oriented four-element antenna with a single 150 kHz broadband receiver. The riometer records the ionospheric absorption of the cosmic radio noise (CNA). In this study, we used the riometer data converted to dB absorption. Thus, a positive (negative) deflection in the riometer trace presented here indicates an increase (a decrease) in absorption intensity. The absorption is used as an indicator of the precipitation of magnetospheric energetic electrons (> 30 keV) into the ionospheric D region.

3. Observations on 7 December 2002

3.1. Solar Wind and Geomagnetic Conditions

[11] Figure 1 shows the overview of the solar wind condition, geomagnetic activity, and ground magnetic pulsation activity for a 12 h interval on 7 December 2002 covering the selected Pc5 event. The shaded rectangles indicate the Cluster-CANOPUS conjunction interval of 1245–1315 UT when the Pc5 event was observed simultaneously in space and on the ground. For most of the 12 h interval, IMF B_x (B_y) was predominantly positive (negative), while IMF B_z was fluctuating within ± 10 nT. The solar wind speed (V_{sw}) began to increase gradually from ~ 500 km s^{-1} around 0700 UT and then reached near ~ 600 km s^{-1} after 1000 UT. The high-speed V_{sw} stream condition remained at least for several hours. The solar wind dynamic pressure (P_{sw}) had fluctuations of ~ 10 – 15 nPa at the leading edge of the high-speed V_{sw} stream. After that, it gradually decreased by ~ 5 nPa as V_{sw} increased. The average upstream solar wind and IMF values for the conjunction interval are as follows: IMF $|B| = 8.0$ nT, IMF $B_x = 6.3$ nT, IMF $B_y = -3.6$ nT, IMF $B_z = 1.9$ nT, $V_{sw} = 587$ km s^{-1} , and $P_{sw} = 5.3$ nPa.

[12] The $SYM-H$ and AU/AL indices are often used as indicators of geomagnetic storm and substorm activities, respectively. The $SYM-H$ index indicated a small geomagnetic storm, which reached the storm maximum at 0839 UT as defined by $SYM-H$ minimum of -43 nT and then recovered to about -20 nT by the end of the interval. Between 1100 UT and 1400 UT, on the other hand, the AL index indicated three successive negative excursions, indicating the presence of substorm activities. The moderate substorm with negative excursion of -517 nT occurred around ~ 1200 UT. Compared with the moderate substorm, the other remaining two substorm activities were relatively small, as characterized by small negative excursions of AL index: -289 nT at ~ 1100 UT and -292 nT at ~ 1300 UT.

[13] We found noticeable Pc5 activity in the magnetic X component at Gillam (GIL, $L=6.2$) in the CANOPUS array for several hours after ~ 1000 UT when GIL was in the

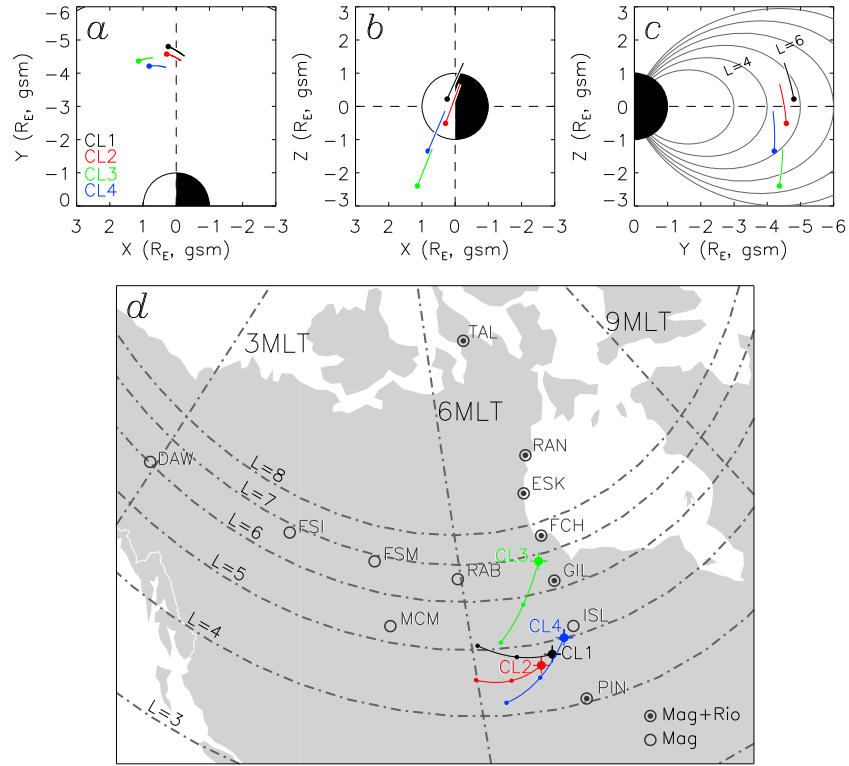


Figure 2. Location of four Cluster spacecraft (CL1: black, CL2: red, CL3: green, CL4: blue) for the interval from 1245 UT to 1315 UT on 7 December 2002, displayed in the (a) XY , (b) XZ , and (c) YZ planes in GSM coordinates. Each filled circle marks each Cluster location at 1245 UT. In Figure 2c, the projections of the reference magnetic field lines at L values from 3.0 to 8.0 (solid curve) are represented. (d) Also displays the Cluster footprints, together with the stations of magnetometers and riometers used in this study. Each large circle marks each satellite footprint at 1245 UT, while the small circles mark the footprints at 1300 UT and 1315 UT.

morning auroral zone. This Pc5 activity is probably associated with high-speed V_{sw} stream of 550 km s^{-1} or more. Such a tendency—i.e., high-speed V_{sw} streams favor the generation of auroral-latitude Pc5 activity in the morning sector—is well known [e.g., *Engebretson et al.*, 1998]. When attention has been paid to the space-ground conjunction interval of 1245–1315 UT, we notice that the Pc5 amplitude at GIL is enhanced by a factor of 1.5–2.0, compared with that during the other intervals. More detailed characteristics of the Pc5 oscillation will be presented in the next section.

3.2. Pc5 in Space and on the Ground

[14] Figures 2a, 2b, and 2c indicate the orbits of four Cluster spacecraft (CL1: black, CL2: red, CL3: green, CL4: blue) in the GSM x - y (left), x - z (center), and y - z (right) planes from 1245 UT to 1315 UT. The solid circle represents each Cluster position at 1245 UT. During this interval, the four Cluster spacecraft were traveling across different L shells of ~ 4.0 – 6.5 , inbound to the equatorial/off-equatorial inner magnetosphere near the dawn terminator. Figure 2d illustrates the ionospheric footprints of Cluster spacecraft mapped into the Northern Hemisphere, together with the CANOPUS magnetometer and NORSTAR riometer stations used in this study. The dash-dotted contours display the L values from 3.0 to 8.0, corresponding to those in Figure 2c. The large solid circle marks the Cluster footprint at 1245 UT, and the two small solid circles mark the footprints at 1300 UT and 1315 UT,

respectively. For most of this 30 min interval, the CL3 footprint passed near GIL ($L=6.2$), and the others fell in a smaller L shell region between Island Lake (ISL, $L=5.2$) and Pinawa (PIN, $L=4.1$).

[15] Figure 3 presents the magnetic and electric field data from all four Cluster spacecraft for 1230–1330 UT on 7 December 2002. Both fields, which are represented in local mean FA coordinates (see section 2), show the poloidal (B_v , E_ϕ) and toroidal (B_ϕ , E_v) modes. ΔB exhibits the time-varying fluctuation in the total magnetic field strength (i.e., compressional mode), defined by subtracting the 15 min running average from the magnetic field strength. The bottom three panels of Figure 3 show position of the satellites in dipole-based coordinates (L value, polar angle, and MLT). During the interval from 1245 UT to 1315 UT, all four Cluster spacecraft observed a monochromatic, compressional Pc5 oscillation in ΔB , with a nearly identical waveform but with a phase shift between satellites. The peak-to-peak amplitude was in the range of 5–10 nT and slightly larger at CL3 than at the other spacecraft. During the same interval, both the poloidal and toroidal modes also showed the corresponding Pc5 oscillations, but the amplitudes strongly depended on the satellite locations. CL3, located at the highest L (5.0–6.5), observed the toroidal Pc5 magnetic field oscillation with the largest peak-to-peak amplitude of 25–45 nT in B_ϕ . We also found that the toroidal Pc5 oscillation at CL3 had a phase shift that B_ϕ led radial electric field

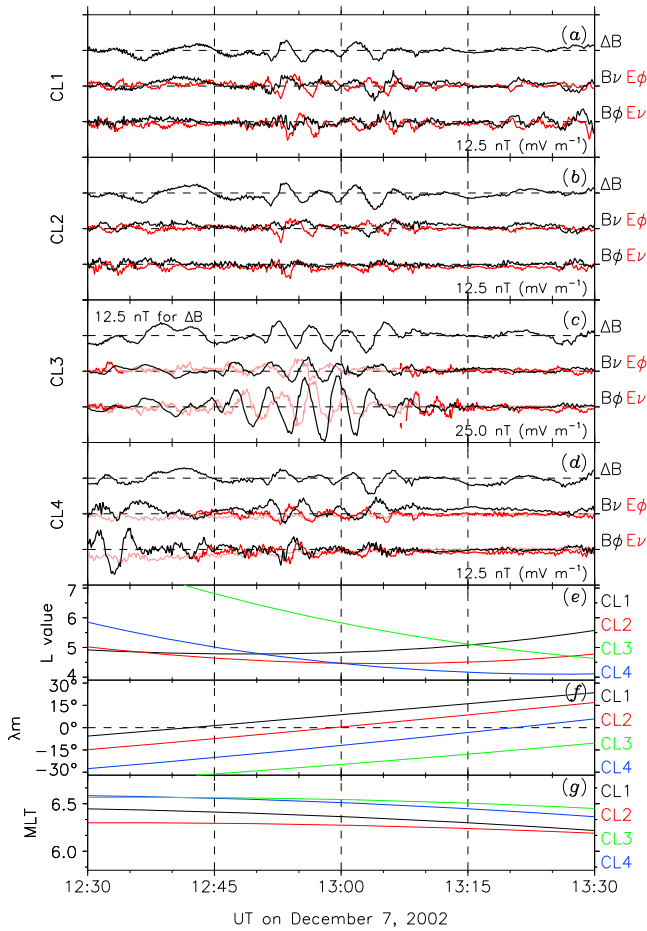


Figure 3. (a–d) The magnetic (black) and electric (red) fields in field-aligned coordinates at four Cluster spacecraft from 1230 UT to 1330 UT on 7 December 2002. The subscript indicates the radial (ν) and azimuthal (ϕ) components. ΔB is defined by subtracting the 15 min running average from the magnetic field strength. Light red curves in Figures 3c and 3d represent the electric field vector calculated from $\mathbf{E} = -(\mathbf{V} \times \mathbf{B})$ using the CIS and FGM instrument data. Note that the tick scale in the Y axis is the same, except the ν and ϕ components of the magnetic and electric fields at CL3. (e–g) L value, polar angle (λ_m), and MLT of the Cluster spacecraft (CL1: black, CL2: red, CL3: green, CL4: blue).

($E\nu$) by almost 90° , as expected from a fundamental standing wave structure [Singer *et al.*, 1982]. The toroidal Pc5 magnetic field oscillation dramatically weakened (peak-to-peak amplitude ≤ 5 nT) at the other CLs located at lower L (4.0–5.0). Also at CL1, we could find approximately 90° phase shift between $B\phi$ and $E\nu$, but unlike CL3, $B\phi$ lagged $E\nu$. For a fundamental standing wave, in general, the phase shift between $B\phi$ and $E\nu$ should be opposite between the Northern and Southern Hemispheres. Therefore, the toroidal Pc5 oscillation at CL1 seemed also to be thought as fundamental standing wave. At CL2 and CL4, the phase relationship between $B\phi$ and $E\nu$ was more complicated or unclear.

[16] Figure 4 presents the power spectra of the ΔB , $B\nu$, and $B\phi$ field oscillations for this event. The spectral analysis confirmed that a narrow-band compressional Pc5 at 4.0 mHz (marked by vertical grey line) existed in the inner magnetosphere.

The monochromatic Pc5 oscillations with an L independent frequency at 4.0 MHz were also obvious in the transverse modes ($B\nu$ and $B\phi$). As mentioned above, both spectral powers were more significant at CL3 than at the others.

[17] The monochromatic Pc5 oscillations seen at Cluster were also observed around the conjugate point of the Cluster spacecraft. As shown in Figure 3, the four Cluster footprints were close to three lower latitude stations (GIL, ISL, and PIN) of the Churchill line magnetometer array. Figure 5 shows the unfiltered magnetic X (red) and Y (blue) component variations at the CANOPUS Churchill line stations for the interval of 1230–1330 UT and the power spectra. For the power spectra, in the case that the X and Y components have the same frequency, we mark the dominant peak with dashed black line. In the case that the X and Y components have different frequencies, the dominant peak of X (Y) component is marked by dashed red (blue) line. During the interval of interest, a clear wave packet of Pc5 oscillation can be seen over a wide latitude range from Fort Churchill (CHU, $L=7.5$) to PIN. The spectral analysis indicated that

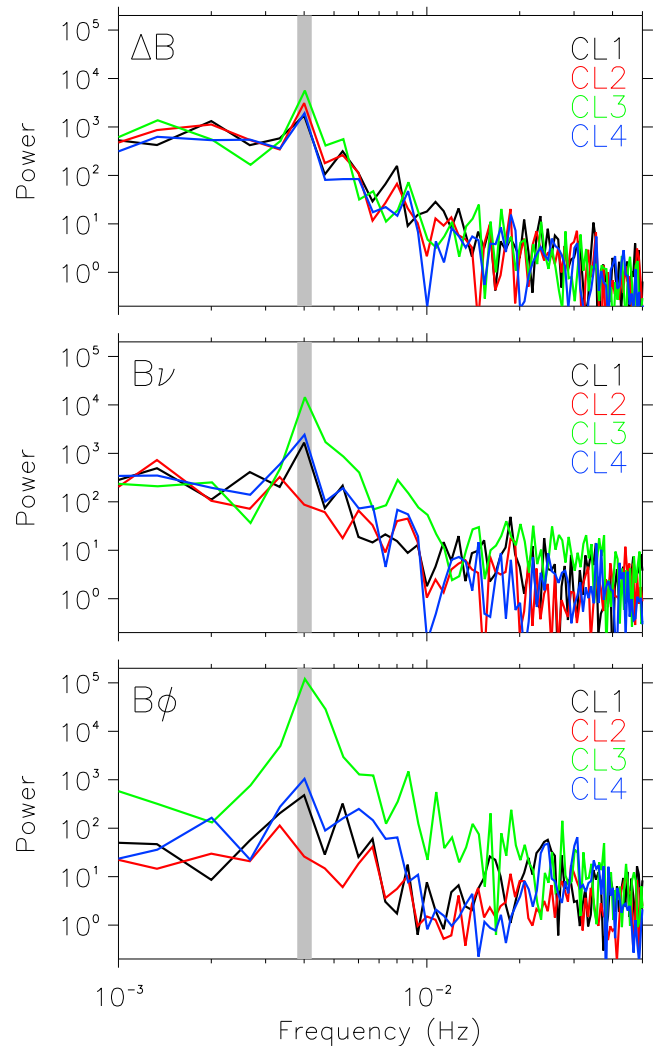


Figure 4. Power spectra of the ΔB , $B\nu$, and $B\phi$ oscillations, calculated for the interval from 1245 UT to 1310 UT when the magnetospheric Pc5 activity was dominant. The thick grey line denotes the 4.0 mHz frequency.

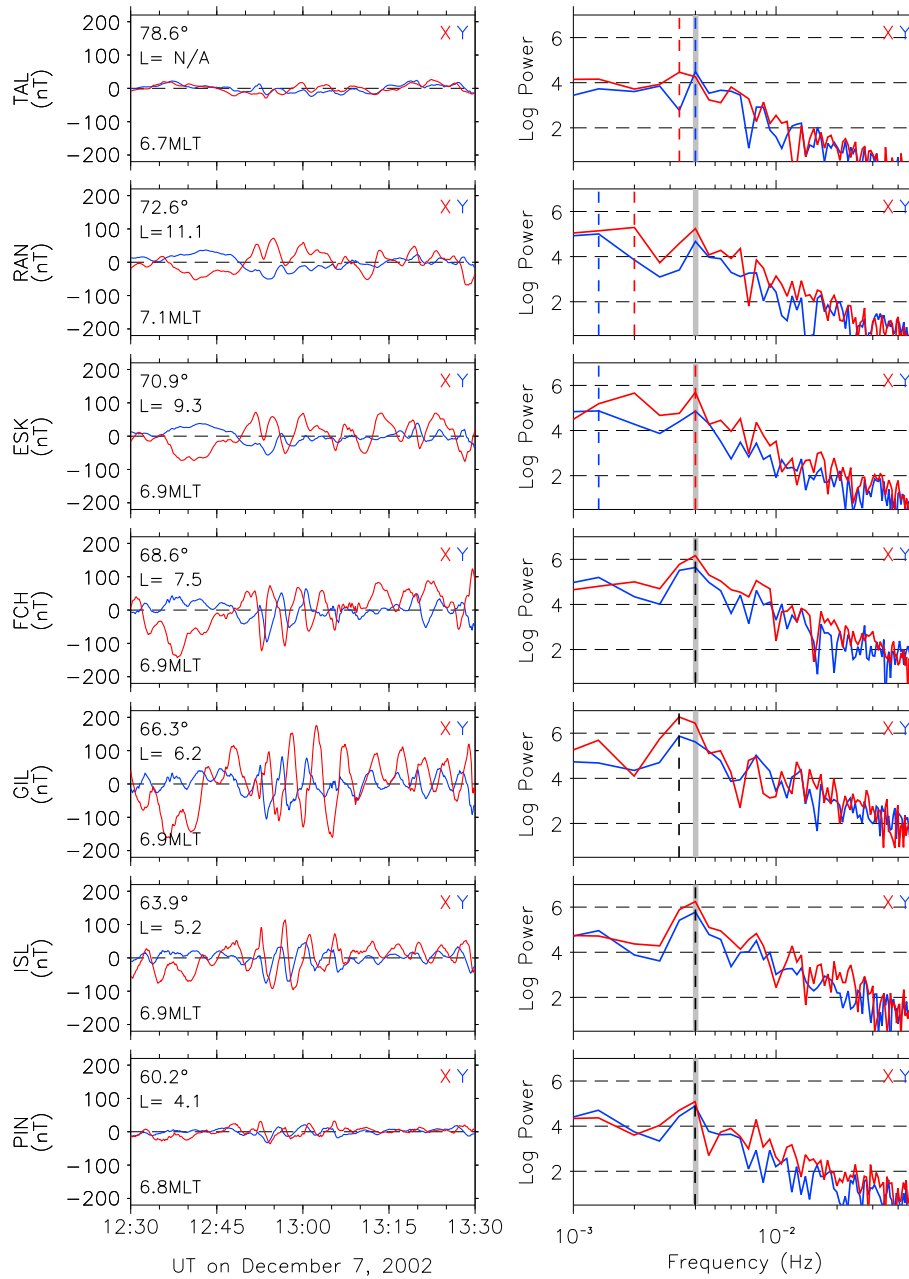


Figure 5. Unfiltered X (red) and Y (blue) component variations in the ground magnetometer data at the CANOPUS Churchill line stations and their power spectra. For reference, the 4.0 mHz frequency is denoted by thick grey line. For the power spectra, in the case that the X and Y components have the same frequency, we mark the dominant peak with dashed black line. In the case that the X and Y components have different frequencies, the dominant peak of X (Y) component is marked by dashed red (blue) line.

the Pc5 oscillations at most of the stations had a significant spectral peak near ~ 4.0 mHz (represented by gray line), matching the main frequency of magnetospheric Pc5 oscillations observed at Cluster. Here it is interesting to note that the spectral power at GIL peaked at slightly lower frequency (~ 3.3 mHz) than that at the other stations, but this puzzling result will be discussed in section 4. The higher-latitude stations, Eskimo Point ($L=9.3$) and Rankin Inlet ($L=11.1$), had the additional lower frequency peaks around 2.0 mHz or lower.

[18] Figure 6 presents the latitudinal profile of the Fourier power and phase for the spectral maxima at 4.0 mHz. The X

component displayed a latitudinal amplitude peak at GIL, and a corresponding phase shift of 180° across the maximum. The latitudinal profile resembles the classical FLR signatures on the ground. The D component amplitude was distributed over a broader latitude range from ISL to CHU, but there was little phase change. The latitudinal profile of ground Pc5 amplitude was consistent with space-based results, indicating the localization of toroidal Pc5 amplitude at CL3 almost magnetically conjugated to GIL. Both space and ground observations suggest that the center of resonance at 4.0 mHz lies near the CL3 orbit, $\sim L=6.0$.

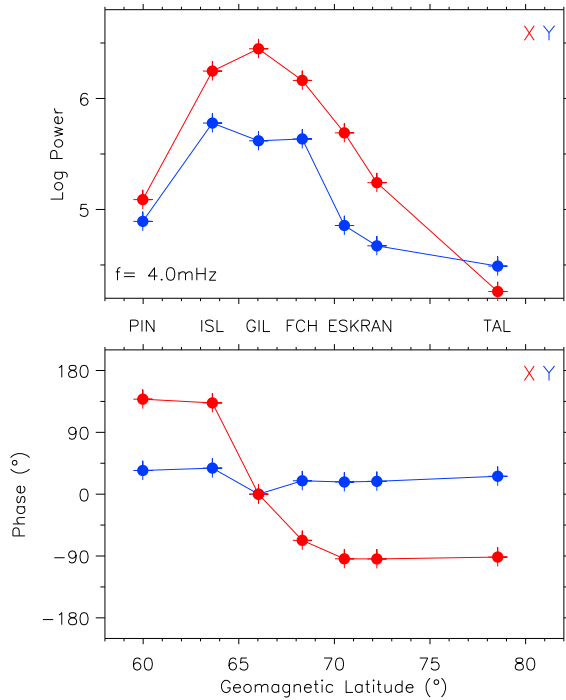


Figure 6. Latitudinal profiles of amplitude and phase estimated from the 4.0 mHz magnetic X (red) and Y (blue) component oscillations at the CANOPUS Churchill line stations.

[19] To determine the azimuthal wave number m , we computed the cross-spectral density between the 4.0 mHz oscillations from two longitudinally spaced station pairs at different L values: Gillam-Rabbit Lake (longitudinal difference: 14.09°) at $L \sim 6.4 \pm 0.2$ and Island Lake-Fort McMurray (longitudinal difference: 24.33°) at $L \sim 5.3 \pm 0.1$. At each station pair, the 4.0 mHz oscillation showed an apparent phase difference for which the wave signal at the eastern station preceded that at the western station. If we assume that the propagation is strictly azimuthal, the result means that the 4.0 mHz oscillation on the ground propagated westward. In addition, using the phase difference and the longitudinal difference at each station pair, we obtained an azimuthal wave number of $m = 4-5$.

3.3. Pc5 Modulation of Energetic Electrons and Chorus Waves

[20] In this section, we present the coordinated space-ground comparisons of Pc5-related modulation using the Cluster energetic electron and plasma wave data and the NORSTAR riometer data. For such comparisons, we use data from two near-conjugate pairs: one is the higher L shell CL3-GIL pair ($L \sim 5.0-6.5$), the other the lower L shell CL4-PIN pair ($L \sim 4.0-5.0$). Figure 7 presents an overview displaying the in situ and ground Pc5-related modulation observations from the CL3-GIL pair. Figure 7a presents the ACE solar wind dynamic pressure (Psw) data time shifted by 53 min, including the time delay of 50 min from ACE to Earth's bow shock (cf. OMNI data) and the additional time delay of 3 min from bow shock to geosynchronous orbit [cf. Jackel et al., 2012]. Figures 7b-7f show the Cluster observations, including the three components of the magnetic field shown in Figure 3c (ΔB : red, B_v : green, B_ϕ : blue),

time-frequency spectrograms of the wave amplitude in the electric and magnetic fields in the frequency range from 100 Hz to 4.0 kHz, energetic electron fluxes in the range of 40–250 keV as labeled, and pitch angle distribution of the 50.5 keV electron flux. The dashed white horizontal line in Figures 7c and 7d represents local $0.1f_{ce}$ (f_{ce} is the local electron cyclotron frequency determined from the measured ambient magnetic field). Figures 7g and 7f show the GIL riometer absorption and magnetometer (X component: red, Y component: blue) observations. Note that there was an unfortunate gap for a few minute interval around ~ 1307 UT in the electron flux data at CL3.

[21] Between 1230 UT and 1330 UT when CL3 was moving across different L shells from the southern middle latitude toward the magnetic equator (see Figure 3), the energetic electron fluxes was gradually increasing. Coincident with the Pc5 oscillation in ΔB (compressional mode) with about four wave cycles, the energetic electron fluxes varied with the same wave cycles. The electron flux modulation was almost in phase across energy channels. The pitch angle distribution of 50.5 keV electron flux at CL3 showed that both precipitating (pitch angles closer to 0° or 180°) and trapped (pitch angles closer to 90°) components were modulated by Pc5. The electron flux was slightly higher in the precipitated component than in the trapped one, by a factor of 1.1–1.4. We also found similar cigar-like pitch angle distribution in the other energy channels (not shown here). For the precipitated component, we also found that the amplitude of Pc5-related electron flux modulation was slightly larger at 50.5 keV than at the other energy channels. As the ionospheric counterpart of the precipitating electron flux modulation observed at CL3, CNA pulsation with peak-to-peak amplitude of 0.4–0.6 dB was recorded with the riometer at GIL.

[22] The STAFF-SA at CL3 observed a banded, intense electromagnetic emission of chorus type between a few hundred Hz and 3.0 kHz, in both time-frequency spectrograms of wave electric and magnetic fields. The central frequency of the banded emission monotonically increased as CL3 approached to the perigee. Such properties resemble “banded chorus” reported by Burtis and Helliwell [1969]. Furthermore, we found a patch-like structure with quasiperiodicity in the banded chorus wave intensity. In particular, the individual intensity patches of chorus waves with frequencies (several hundreds Hz to 2 kHz) above $0.1f_{ce}$ are likely to positively correlate with the electron flux modulation by Pc5.

[23] Figures 7g and 7h show good correspondence between the CNA pulsation and the enhanced Pc5 magnetic pulsation at GIL. In contrast, before and after the interval of 1245–1315 UT, such correspondence was poor, which means that the Pc5 magnetic pulsation was not accompanied by a corresponding CNA pulsation. This implies that the generation mechanism of Pc5 oscillation for the interval of 1245–1315 UT was different from that for the other intervals.

[24] Figure 8, which is the same format as Figure 7, indicates the comparison of the CL4-PIN observations. Similar to the CL3-GIL pair, the CL4-PIN pair at lower L of $\sim 4.0-5.0$ also indicates apparent link between Pc5 oscillations/modulations in space and on the ground. The Pc5 oscillation in ΔB was accompanied by the modulation of energetic electron flux and chorus wave intensity (above $0.1f_{ce}$: > 2 kHz) with a

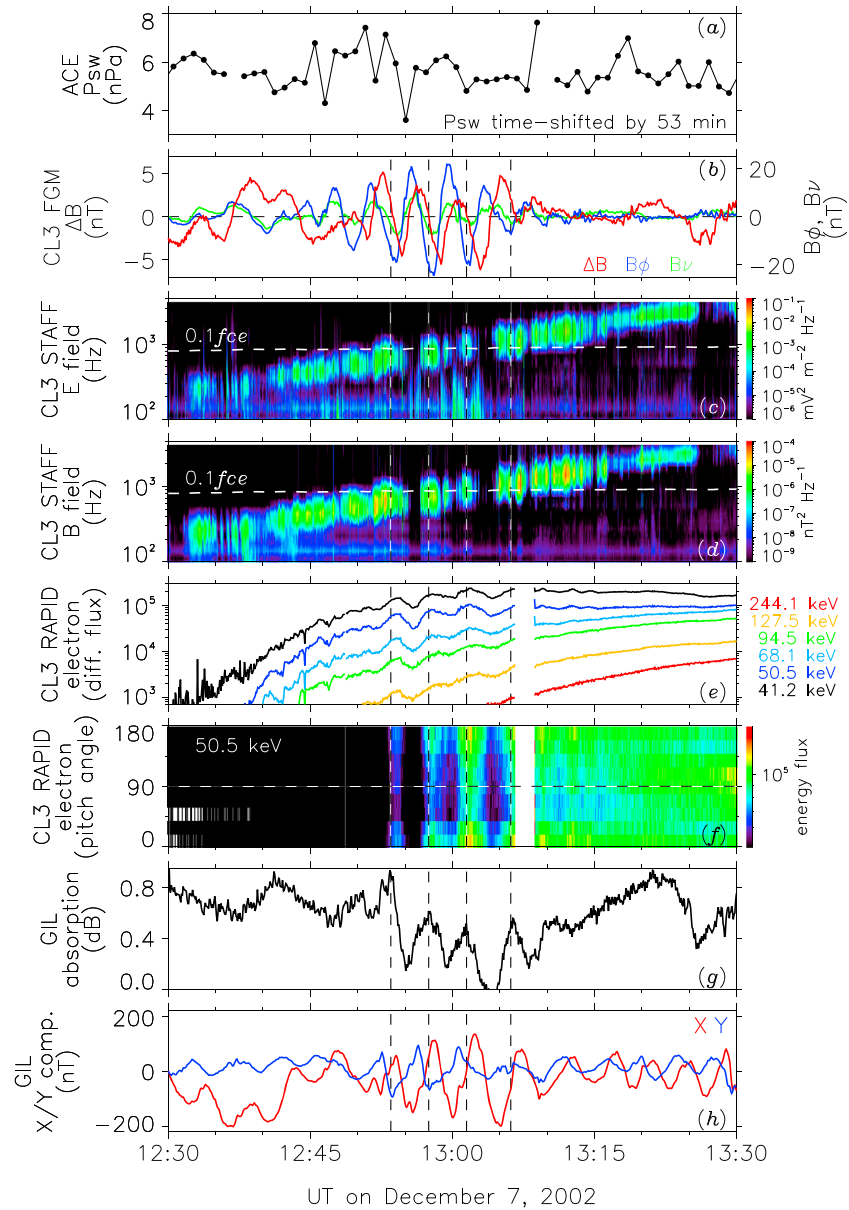


Figure 7. An overview of Pc5 modulation observed simultaneously at Cluster 3 and at Gillam. (a) Temporal variation of solar wind dynamic pressure (Psw) at ACE time shifted by 53 min, (b) the magnetic field perturbations (ΔB : red, $B\nu$: green, $B\phi$: blue) at Cluster 3, time-frequency spectrograms of (c) wave electric and (d) magnetic fields, (e) omnidirectional electron fluxes at the six channels in the range of 40–250 keV, (f) pitch angle distribution of 50.5 keV electron flux, temporal variations of (g) riometer absorption, and (h) magnetometer at Gillam. The dashed white horizontal lines in Figures 7c and 7d represent $0.1f_{ce}$. Dashed vertical lines are drawn at four positive peaks in absorption.

similar temporal variation. Here when considering the theoretical resonance condition of chorus wave–electron interaction in a quasiuniform equatorial plane, it is expected that the modulation of precipitating energetic electron fluxes could be efficient at lower energy channel at CL4 than CL3, because the chorus wave frequency was higher at CL4 than CL3. However, we could not find such an expected difference between CL4 and CL3, and rather at CL4 the modulation was strong at slightly higher energy channel (68.1 keV). In addition, the electron flux modulation at CL4 positively correlated with the CNA pulsation at PIN. The CNA pulsation at PIN resembled that at GIL, but the amplitude (~ 0.1 – 0.2 dB) was less than half of that

at GIL. Both CNA and magnetic pulsations at PIN had good correspondence during the interval of interest.

4. Discussion

[25] In this case study we investigated the modulation of electron precipitation (> 40 keV) by Pc5 magnetic pulsations using observations made by the Cluster spacecraft and near the spacecraft footprint by the NORSTAR/CANOPUS ground-based experiments. As demonstrated in the previous section, the monochromatic compressional Pc5 at 4.0 mHz was dominated in the $L \sim 4.0$ – 6.5 region covered by Cluster.

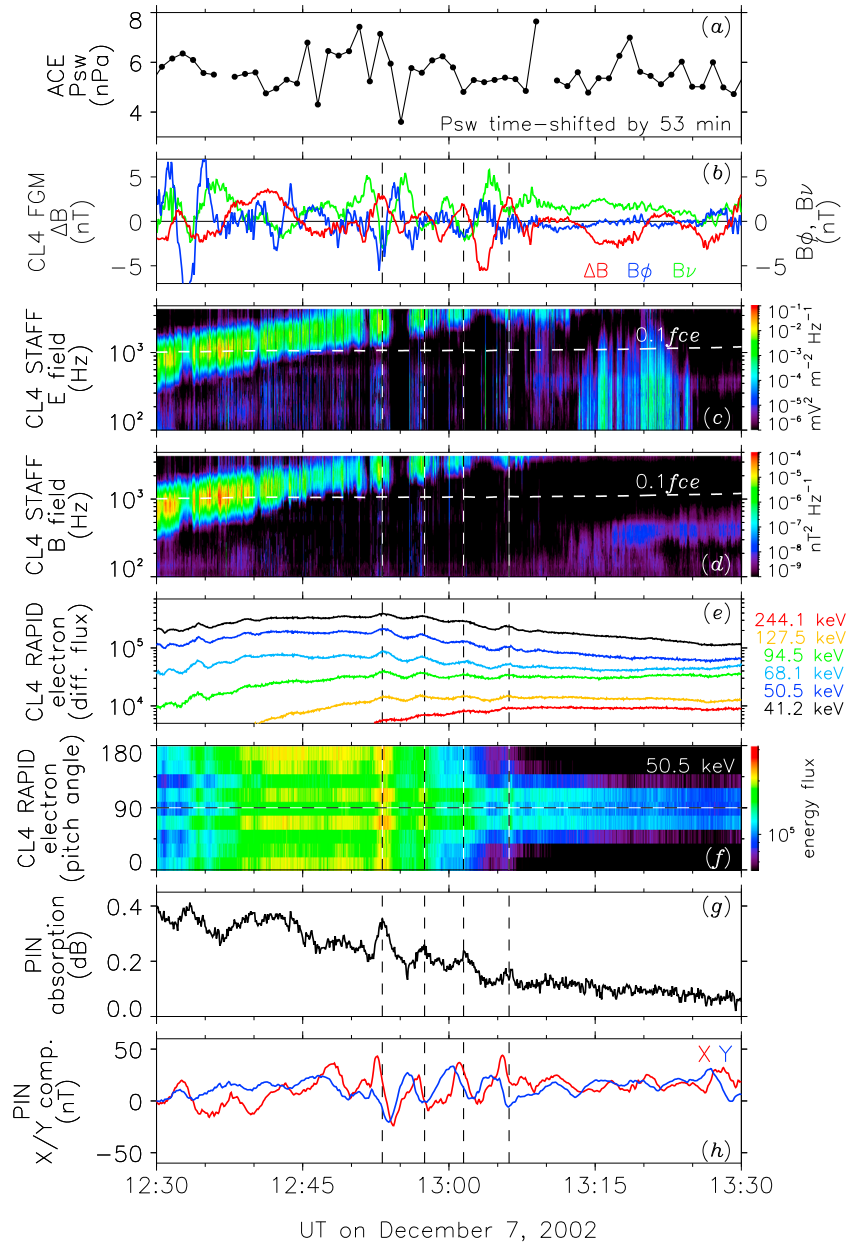


Figure 8. Same as Figure 7 but for simultaneous observations at Cluster 4 and at Pinawa.

Another interesting point is that the compressional Pc5 with several wave cycles was accompanied by similar modulations at ~ 4.0 mHz of chorus wave emission, electron flux, and energetic electron precipitation, as well as by the resonant toroidal Pc5 detected commonly in space and on the ground. Especially, the 4.0 mHz CNA pulsation (i.e., the modulated precipitation of energetic electrons) occurred for the only interval when the compressional Pc5 was dominated. Most of the space-ground observational results reasonably agree with the *Coroniti and Kennell* [1970] theory that describes a possible causal relationship among compressional magnetic pulsations in the magnetosphere, whistler mode chorus waves, and precipitation of energetic electrons.

[26] From the CL3-GIL observations in Figure 7, however, we found that the compressional Pc5 at CL3 apparently preceded the Pc5-related modulations of chorus wave emission, electron flux, and energetic electron precipitation by $\sim 90^\circ$.

This feature cannot be explained by the theory of *Coroniti and Kennell* [1970], predicting that all of them vary in phase as seen in the CL4-PIN observations in Figure 8. The exact reason for this discrepancy is still not clear, but the CL3-GIL observations imply that there are other mechanisms operating concurrently, at least L shells near CL3-GIL.

[27] In order to resolve the above discrepancy, as an alternative, it would be worthwhile to consider an incompressible (i.e., shear Alfvén mode) oscillation of the magnetic field in the magnetosphere and its possible roles in modulating energetic electrons. Indeed, while the compressional Pc5 was dominated in the magnetosphere, the resonant toroidal Pc5 with large amplitude was observed at CL3 crossing the outer L shells ($5.0 < L < 6.5$). Consistent with the CL3 observations, GIL closer to the CL3 footprint indicated the well-known resonance structure, with a local peak in amplitude and a phase shift of $\sim 180^\circ$ across the resonant latitude.

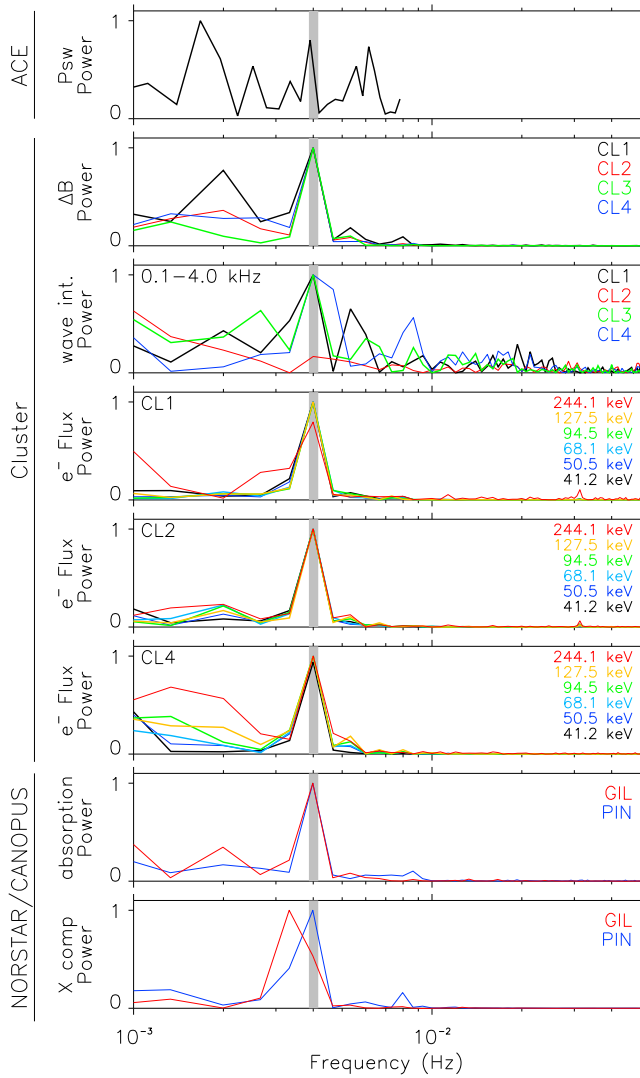


Figure 9. Normalized power spectra in the time-shifted ACE solar wind dynamic pressure (Psw), Cluster magnetic field strength, Cluster 0.1–4.0 kHz chorus wave emission, Cluster electron energy fluxes in the range of 40–250 keV, and ground-based riometer and magnetometer data at Gillam and Pinawa. The thick grey line represents the 4.0 mHz frequency.

In Figure 7, we found that the large-amplitude toroidal Pc5 at CL3 was coincident almost out-of-phase with the modulations of chorus wave emission and energetic electron fluxes. In addition, the amplitude of CNA pulsation was much stronger at GIL than that at the other higher-latitude/lower latitude stations. These intriguing CL3-GIL observations around the FLR region imply that the Pc5 FLR oscillation is linked in some way to the modulation of precipitating energetic electrons. Some possible FLR-related processes responsible for the CNA pulsation have been proposed, such as periodic acceleration and precipitation of electrons by the parallel electric field of a kinetic Alfvén wave in the FLR [Nosé *et al.*, 1998] or modulation of the field-aligned potential drop by the interaction of Alfvén waves with the auroral acceleration region [Fedorov *et al.*, 2004].

[28] As evident in Figures 7g and 7h, we emphasize here that not all Pc5 magnetic field oscillations on the ground

(i.e., toroidal Pc5) were accompanied by a corresponding CNA pulsation. As mentioned above, the CNA pulsation became obvious only during the remarkable compressional Pc5. Therefore, the FLR-related mechanism(s) cannot completely explain the generation of CNA pulsation, but the FLR-effects may play an additional role at least around the resonant shell.

[29] When considering the phase difference between ground Pc5 and CNA pulsations, one would expect to see ground magnetic pulsations following the precipitation modulation (CNA pulsation) due to the different traveltimes of electrons (a timescale of seconds) and Alfvén waves (a time of the order of a minute). Here the approximate Alfvén traveltime from the equatorial plane to one ionosphere was estimated using a simple time-of-flight approach for standing Alfvén waves [Warner and Orr, 1979]. From Figures 7g and 7h, we found that at GIL the ground magnetic Pc5 in the X component apparently lagged the CNA pulsation by $\sim 90^\circ$. It seems reasonable to explain the phase difference at GIL in terms of the difference in traveltime. At PIN, on the other hand, the magnetic Pc5 in the X component preceded the concurrent CNA pulsation. For the phase of magnetic Pc5 at PIN, we have to take into account the FLR effect. Whereas the CNA pulsation at PIN occurred almost simultaneously with the modulation of precipitating energetic electrons by the compressional Pc5 at CL4, as seen in Figure 6 the magnetic Pc5 at PIN underwent an apparently preceding phase shift through the resonant region.

[30] For the generation of CNA pulsations, the preexisting energetic electron population would be required to be sufficient in the inner magnetosphere. It is generally thought that the substorm-related particle injection around midnight is an important seed of the elevated energetic electron flux in the dawnside magnetosphere, because such injected electrons drift eastward toward dawn. For our event, the AL index indicated two successive substorm activities: a moderate substorm (AL index of -517 nT peaking at ~ 1200 UT) about a few hours before the present Pc5 event and a small substorm (AL index of -292 nT) just during the event. In fact, the LANL satellite(s) around midnight observed injections of energetic electrons during the intervals of two substorm activities (not shown here). These results allow us to suggest that such substorm-related injections could contribute to ensuring a stable supply of energetic electrons in the dawnside inner magnetosphere, suitable for the generation of CNA pulsations.

[31] The resonant Pc5 signature at 4.0 mHz was commonly evident from both space and ground measurements. The space-ground Pc5 features studied here are similar in many respects to the coordinated GOES 7 and CANOPUS observations of Pc5 oscillations by Ziesolleck *et al.* [1996], indicating that the ground stations and satellite had the same discrete spectra and that these signals were associated with resonances. In our data, however, we encountered a puzzling feature in the ground-based results, why the Pc5 spectral power at GIL peaked apparently at lower frequency (~ 3.3 mHz, see Figure 5). Such a frequency shift cannot be readily predicted in the framework of the FLR theory. There exists a possible explanation for the frequency shift of spectral power at GIL, although somewhat speculative. When the local magnetic field lines respond to a monochromatic oscillatory driver imposed over a wide range of latitudes

by some source mechanism, the field lines will mainly oscillate at the driving frequency. However, if the local resonant eigenfrequency at a particular observation point is very close to (but slightly different from) the driving frequency, the resulting field line oscillation will be strong at the local eigenfrequency as well as driving frequency to maintain the field line oscillation. As a result, the spectral power peak at the observation point might apparently be formed in the region of a frequency shift relative to the driving frequency, as seen at GIL.

[32] While the strong Pc5 was evident at CL3 ($L \sim 5.0\text{--}6.5$), the CIS-HIA instrument at CL3 observed the ion density (with energy range of 40 eV–40 keV) profile monotonically increasing from a few cm^{-3} to $\sim 30 \text{ cm}^{-3}$ (not shown). On the other hand, the electron density inferred from the spacecraft potential data ($n_e = (0.08U)^{-1.78}$), where U is spacecraft potential [cf. *Moullard et al.*, 2002], was $5\text{--}15 \text{ cm}^{-3}$. Such a plasma density is not as dense as expected for the plasmasphere ($\sim 100 \text{ cm}^{-3}$) but relatively higher than that in the plasma sheet. These results suggest that the resonant toroidal Pc5, dominated in L shell of ~ 6.0 , may be excited via a coupling process with the concurrent 4.0 mHz compressional Pc5 just outside the plasmopause.

[33] Identification of the source mechanisms is one of the important topics in studies of magnetospheric pulsations. Generation mechanisms of compressional Pc5 oscillations are mainly divided into two: internal process and external process. The internally excited compressional Pc5 is commonly explained in terms of the drift-mirror mode [*Hasegawa*, 1969]. Drift-mirror modes are compressional modes that are excited by plasma pressure anisotropy, and they are characterized by an antiphase relationship between the magnetic and plasma pressures and by a large azimuthal wave number ($m > 20$). The compressional Pc5 driven by drift-mirror mode tends to occur preferentially in the outer dawn/dusk equatorial magnetosphere at a radial distance larger than $8 R_E$, up to the magnetopause, especially in the high plasma beta region ($\beta > 1$, i.e., thermal plasma pressure is dominant) [e.g., *Zhu and Kivelson*, 1991]. Contrary to such characteristics, we observed the compressional Pc5 magnetic field oscillations in the inner magnetosphere (L shells of $\sim 4.0\text{--}6.5$) that was dominated by the magnetic pressure ($\beta < 1$). Also, the ground Pc5 had a small m number of 4–5, and it apparently propagated westward, as estimated from the longitudinally separated station pairs. These space- and ground-based results allow us to rule out the possibility that an internal process, such as drift mirror mode instability, drives the observed compressional Pc5.

[34] On the other hand, quasiperiodic magnetopause motions by Kelvin-Helmholtz instability (KHI) at the magnetopause boundary and standing or forced magnetospheric oscillations by solar wind or magnetosheath pressure (referred to as “external pressure”) variations are obvious candidates for the external generation mechanism of compressional Pc5 oscillation in the magnetosphere.

[35] We note that the solar wind speed was moderately fast ($\sim 580 \text{ km s}^{-1}$) for the interval of this Pc5 event. Such a moderate solar wind stream retains potential to drive some magnetopause motions through KHI. Although the KHI-excited magnetopause motions are a possible driver for the observed magnetospheric compressional Pc5, it has still been unclear how the KHI-related unstable waves at the magnetopause

boundary excite a monochromatic compressional Pc5 inside the magnetosphere as observed at CLs.

[36] Another candidate is the external pressure impulse(s)/variation. It is thought that an external pressure impulse can drive the compressional oscillations of the magnetosphere with discrete eigenfrequencies, known as global modes or cavity/waveguide modes [*Kivelson and Southwood*, 1986; *Samson et al.*, 1992]. At least occasionally, on the other hand, a class of magnetospheric compressional oscillations is directly driven by inherent oscillations in the solar wind dynamic pressure (Psw) [e.g., *Sarafopoulos*, 1995; *Kepko et al.*, 2002; *Motoba et al.*, 2003]. In this case, the compressional oscillations resemble the behavior of the global cavity/waveguide modes, but their frequencies are determined by periodic Psw forcing (i.e., forced oscillations). Here we examined the Psw data at ACE to distinguish whether the 4.0 mHz compressional Pc5 at CLs result from the forced oscillation or the standing compressional oscillation of the magnetosphere. As shown in Figures 7a and 7b and 8a and 8b, the first cyclic change of time-shifted Psw perturbation at ACE appears to be fairly similar to that of the compressional (ΔB) variation at CL3/CL4, but both Psw and ΔB variations were not always identical through a whole interval. In order to further investigate whether the observed Psw fluctuations could potentially drive the compressional Pc5 at 4.0 mHz in the magnetosphere, we have calculated the Psw spectrum from the time-shifted ACE data. Figure 9 shows a spectral analysis of the time-shifted Psw, together with data from the Cluster and NORSTAR/CANOPUS instruments. The thick grey line denotes the 4.0 mHz frequency. From Figure 9, it was found that most of the magnetospheric and ionospheric magnetic fields and electron fluxes and magnetospheric chorus waves had a dominant spectral peak near ~ 4.0 mHz. In contrast, the Psw fluctuation had several spectral peaks, in which the largest peak was at 1.67 mHz, and a secondary peak was at 3.91 mHz. Considering that the Psw spectral power near ~ 4.0 mHz was not prominent in the ACE data, the ACE observation would make it hard to explain that the Psw oscillation directly excited the compressional Pc5 at CLs. Even in the absence of the corresponding Psw oscillation at ACE, however, we cannot completely rule out the possibility of the forced magnetospheric oscillation, i.e., the magnetospheric compressional oscillations might be produced by external pressure fluctuation associated with the bow shock [e.g., *Fairfield et al.*, 1990], not in the solar wind. The exact generation mechanism responsible for the monochromatic compressional Pc5 at CLs remains still unknown, but our limited data allow us to speculate that the compressional Pc5 was driven by any of external source mechanisms discussed above.

5. Summary

[37] In this study, we have presented the coordinated Cluster and ground-based observations of the Pc5 modulation of energetic electrons in the dawnside L shells of $\sim 4.0\text{--}6.5$ on 7 December 2002. Such a conjunction of space- and ground-based instrumentations provides, for the first time, close linkages between the in situ measurements of compressional Pc5, energetic electron flux and chorus wave, and the ground-based measurement of CNA pulsation. These space-ground observations reasonably support the generation process of

CNA pulsations proposed by *Coroniti and Kennell* [1970], in which a compressional magnetic pulsation in the magnetosphere modulates the growth rate of the chorus waves and consequently modulates the precipitation of energetic electrons. However, some space-ground observations around the resonance shell suggest a possibility that some additional contributions to the modulation of electron precipitation may also come from the effects of the resonant Pc5 oscillation. More investigations will be required for understanding how FLRs contribute to the modulated precipitation of energetic electrons.

[38] **Acknowledgments.** Work at JHU/APL was supported by the NSF grants (1003580 and NSF1104338) and NASA grants (NNX10AK93G and NNX12AJ52G). We would like to acknowledge the Cluster Active Archive and the instrument teams for providing all Cluster instrument data used in this study. The CANOPUS instrument array (now the CANOPUS magnetometers and riometers are maintained and operated by CARISMA and NORSTAR, respectively) was supported by the Canadian Space Agency. We thank E. Spanswick (University of Calgary) for providing helpful advice on the riometer data. The ACE and OMNI data used in this study were made publicly available through CDAWeb. The geomagnetic activity data (*SYM-H* and provisional *AU/AL* indices) were obtained from the Kyoto Data Center.

[39] Robert Lysak thanks Martin Connors and two anonymous reviewers for their assistance in evaluating this paper.

References

- Baker, J. B., E. F. Donovan, and B. J. Jackel (2003), A comprehensive survey of auroral latitude Pc5 pulsation characteristics, *J. Geophys. Res.*, *108*(A10), 1384, doi:10.1029/2002JA009801.
- Balogh, A., et al. (2001), The Cluster magnetic field investigation: Overview of in-flight performance and initial results, *Ann. Geophys.*, *19*, 1207–1217, doi:10.5194/angeo-19-1207-2001.
- Barcus, J. R., and T. J. Rosenberg (1965), Observations on the spatial structure of pulsating electron precipitation accompanying low frequency hydromagnetic disturbances in the auroral zone, *J. Geophys. Res.*, *70*, 1707–1716.
- Burtis, W. J., and R. A. Helliwell (1969), Banded chorus—A new type of VLF radiation observed in the magnetosphere by OGO 1 and OGO 3, *J. Geophys. Res.*, *74*, 3002–3010.
- Chen, L., and A. Hasegawa (1974), A theory of long-period magnetic pulsations. I. Steady state excitation of field line resonance, *J. Geophys. Res.*, *79*, 1024.
- Cornilleau-Wehrin, N., et al. (2003), First results obtained by the Cluster STAFF experiment, *Ann. Geophys.*, *21*, 437–456.
- Coroniti, F. V., and C. F. Kennell (1970), Electron precipitation pulsations, *J. Geophys. Res.*, *75*, 1279–1289.
- Engbreton, M., K.-H. Glassmeier, M. Stellmacher, W. J. Hughes, and H. Lühr (1998), The dependence of high-latitude PcS wave power on solar wind velocity and on the phase of high-speed solar wind streams, *J. Geophys. Res.*, *103*(A11), 26,271–26,283, doi:10.1029/97JA03143.
- Fairfield, D. H., W. Baumjohann, G. Paschmann, H. Lühr, and D. G. Sibeck (1990), Upstream pressure variations associated with the bow shock and their effects on the magnetosphere, *J. Geophys. Res.*, *95*(A4), 3773–3786, doi:10.1029/JA095iA04p03773.
- Fedorov, E., V. Pilipenko, M. J. Engebretson, and T. J. Rosenberg (2004), Alfvén wave modulation of the auroral acceleration region, *Earth Planets Space*, *56*, 649–661.
- Gustafsson, G., et al. (2001), First results of electric field and density observations by Cluster EFW based on initial months of operation, *Ann. Geophys.*, *19*, 1219–1240.
- Hasegawa, A. (1969), Drift mirror instability in the magnetosphere, *Phys. Fluids*, *12*, 2642.
- Jackel, B. J., B. McKiernan, and H. J. Singer (2012), Geostationary magnetic field response to solar wind pressure variations: Time delay and local time variation, *J. Geophys. Res.*, *117*, A05203, doi:10.1029/2011JA017210.
- Kennel, C. F., and H. E. Petschek (1966), Limit on stably trapped particle fluxes, *J. Geophys. Res.*, *71*, 1–28.
- Kepko, L., H. E. Spence, and H. J. Singer (2002), ULF waves in the solar wind as direct drivers of magnetospheric pulsations, *Geophys. Res. Lett.*, *29*(8), 1197, doi:10.1029/2001GL014405.
- Kimura, I. (1974), Interrelation between VLF and ULF emissions, *Space Sci. Rev.*, *16*, 389–411.
- Kivelson, M. G., and D. J. Southwood (1986), Coupling of global magnetospheric MHD eigenmodes to field line resonances, *J. Geophys. Res.*, *91*(A4), 4345–4351, doi:10.1029/JA091iA04p04345.
- Lam, M. M., P. B. Horne, N. P. Meredith, S. A. Glauert, T. Moffat-Griffin, and J. C. Green (2010), Origin of energetic electron precipitation > 30 keV into the atmosphere, *J. Geophys. Res.*, *115*, A00F08, doi:10.1029/2009JA014619.
- Mann, I. R., et al. (2008), The upgraded CARISMA magnetometer array in the THEMIS era, *Space Sci. Rev.*, *141*, 413–451, doi:10.1007/s11214-008-9457-6.
- Manninen, J., N. G. Kleimenova, O. V. Kozyreva, and T. Turunen (2010), Pc5 geomagnetic pulsations, pulsating particle precipitation, and VLF chorus: Case study on 24 November 2006, *J. Geophys. Res.*, *115*, A00F14, doi:10.1029/2009JA014837.
- Motoba, T., T. Kikuchi, T. Okuzawa, and K. Yumoto (2003), Dynamical response of the magnetosphere-ionosphere system to a solar wind dynamic pressure oscillation, *J. Geophys. Res.*, *108*(A5), 1206, doi:10.1029/2002JA009696.
- Moullard, O., A. Masson, H. Laakso, M. Parrot, P. Décréau, O. Santolik, and M. Andre (2002), Density modulated whistler mode emissions observed near the plasmopause, *Geophys. Res. Lett.*, *29*(20), 1975, doi:10.1029/2002GL015101.
- Ni, B., R. M. Thorne, Y. Y. Shprits, and J. Bortnik (2008), Resonant scattering of plasma sheet electrons by whistler-mode chorus: Contribution to diffuse auroral precipitation, *Geophys. Res. Lett.*, *35*, L11106, doi:10.1029/2008GL034032.
- Nosé, M., T. Iyemori, M. Sugiura, J. A. Slavin, R. A. Hoffman, J. D. Winningham, and N. Sato (1998), Electron precipitation accompanying Pc 5 pulsations observed by the DE satellites and at a ground station, *J. Geophys. Res.*, *103*(A8), 17,587–17,604, doi:10.1029/98JA01187.
- Olson, J. V., G. Rostoker, and G. Olchowy (1980), A study of concurrent riometer and magnetometer variations in the Pc4-5 pulsation band, *J. Geophys. Res.*, *80*, 1695–1702.
- Paquette, J. A., D. L. Matthews, T. L. Rosenberg, L. J. Lanzerotti, and U. S. Inan (1994), Source regions of long-period pulsation events in electron precipitation and magnetic fields at South Pole Station, *J. Geophys. Res.*, *99*, 3869–3877.
- Poulter, E. M., and E. Nielsen (1982), The interpretation of ground-based observations of energetic electron fluxes modulated by Pc5 hydromagnetic oscillations, *J. Geophys. Res.*, *87*, 2549–2552.
- Reid, J. S. (1976), An ionospheric origin for Pi1 micropulsations, *Planet. Space Sci.*, *24*, 705–710.
- Rème, H., et al. (2001), First multispacecraft ion measurements in and near the Earth's magnetosphere with the identical Cluster ion spectrometry (CIS) experiment, *Ann. Geophys.*, *19*, 1303–1354.
- Rosenberg, T. J., L. J. Lanzerotti, C. G. MacLennan, and C. Evans (1979), Impulsive, quasi-periodic variations in ionospheric absorption of cosmic radio noise, *J. Geomagn. Geoelectr.*, *31*, 585–597.
- Rostoker, G., et al. (1995), CANOPUS—A ground-based instrument array for remote sensing the high latitude ionosphere during the ISTEP/GGS program, *Space Sci. Rev.*, *71*, 743–760.
- Samson, J. C., B. G. Harold, J. M. Ruohoniemi, R. A. Greenwald, and A. D. M. Walker (1992), Fieldline resonance associated with MHD waveguides in the magnetosphere, *Geophys. Res. Lett.*, *19*, 441–444.
- Sarafopoulos, D. V. (1995), Long duration Pc 5 compressional pulsations inside the Earth's magnetotail lobes, *Ann. Geophys.*, *13*, 926–937, doi:10.1007/s00585-995-0926-x.
- Sato, N., S. Shibuya, K. Maezawa, Y. Higuchi, and Y. Tonegawa (1985), CNA pulsations associated with quasi-periodic VLF emissions, *J. Geophys. Res.*, *90*, 10,968–10,974.
- Singer, H. J., W. J. Hughes, and C. T. Russell (1982), Standing hydromagnetic waves observed by ISEE 1 and 2: Radial extent and harmonic, *J. Geophys. Res.*, *87*(A5), 3519–3529, doi:10.1029/JA087iA05p03519.
- Southwood, D. J. (1974), Some features of field line resonances in the magnetosphere, *Planet. Space Sci.*, *22*, 483.
- Spanswick, E., E. Donovan, and G. Baker (2005), Pc5 modulation of high energy electron precipitation: Particle interaction regions and scattering efficiency, *Ann. Geophys.*, *23*, 1533–1542.
- Takahashi, K., R. W. McEntire, A. T. Y. Lui, and T. A. Potemra (1990), Ion flux oscillations associated with a radially polarized transverse Pc5 magnetic pulsation, *J. Geophys. Res.*, *95*(A4), 3717–3731.
- Wamer, M. R., and D. Orr (1979), Time of flight calculations for high-latitude geomagnetic pulsations, *Planet. Space Sci.*, *27*, 679–689.
- Wilken, B., et al. (2001), First results from the RAPID imaging energetic particle spectrometer on board Cluster, *Ann. Geophys.*, *19*, 1355–1366.
- Zhu, X., and M. G. Kivelson (1991), Compressional ULF waves in the outer magnetosphere: I. Statistical study, *J. Geophys. Res.*, *96*(A11), 19,451–19,467, doi:10.1029/91JA01860.
- Ziesolleck, C. W. S., Q. Feng, and D. R. McDiarmid (1996), Pc 5 ULF waves observed simultaneously by GOES 7 and the CANOPUS magnetometer array, *J. Geophys. Res.*, *101*(A3), 5021–5033, doi:10.1029/95JA02989.